Characterization of a Urea Induced Molten Globule Intermediate State of Glutaminyl-tRNA Synthetase from *Escherichia coli*†

Biplab K. Das, Tista Bhattacharyya, and Siddhartha Roy*

Department of Biophysics, Bose Institute, P1/12, C.I.T. Scheme VII M, Calcutta 700 054, India

Received October 17, 1994; Revised Manuscript Received January 24, 1995®

ABSTRACT: The urea-induced unfolding of glutaminyl-tRNA synthetase, a multidomain protein, has been studied by equilibrium and kinetic methods, using chemical modification, fluorescence, and CD spectroscopy. The far-UV CD, fluorescence, and sulfhydryl reactivity clearly demonstrated the existence of a stable intermediate state at around 2 M urea. The intermediate showed higher binding of 1-anilino-8-naphthalenesulfonic acid. Furthermore, near-UV CD study of the intermediate showed significantly disrupted tertiary structure with only a small change in the secondary structure, which is a characteristic of molten globule states. The activation energies ($\Delta G^{\ddagger}$) calculated from unfolding kinetics monitored by CD and fluorescence suggest that the intermediate state may be separated from the native and the unfolded state by high activation energy barriers.

Characterization of different intermediate states in the process of protein folding has attracted considerable interest in the last three decades. Recently, much attention has been devoted to a class of compact intermediates called molten globules (Ptitsyn, 1987, 1992; Ptitsyn *et al.*, 1990; Dolgikh *et al.*, 1985; Kuwajima, 1989; Baum *et al.*, 1989; Baldwin, 1991; Christensen & Pain, 1991; Dobson, 1992; Lehrman *et al.*, 1991; Palleros *et al.*, 1993). This state is characterized by native-like secondarly structure, disordered tertiary structure, and much higher binding of hydrophobic fluorescent probes such as ANS[1] (Ptitsyn *et al.*, 1990; Khurana & Udgaonkar, 1993; Ewbank & Creighton, 1991; Mitaku *et al.*, 1991). The transient nature of these intermediates in the folding process makes it difficult to study them, and much effort has been made to obtain the molten globule states under equilibrium conditions. It has been observed that mild denaturing conditions such as low urea or guanidine hydrochloride concentrations, slightly elevated temperatures, or moderately acidic or alkaline pH induces molten globule-like states in many proteins (Damaschun *et al.*, 1986; Ptitsyn, 1987; Goto *et al.*, 1990; Jeng & Englander, 1991; Fink *et al.*, 1993). Molten globule states induced by these denaturing conditions may be somewhat different (Nozaka *et al.*, 1978; Dolgikh *et al.*, 1981; Gast *et al.*, 1986; Permyakov *et al.*, 1991; Fink *et al.*, 1991).

Many of the molten globule states that are characterized are in small and medium sized proteins (Jagannadham & Balsubramanian, 1985; Kim & Kim, 1986; Uversky *et al.*, 1992; Jeng *et al.*, 1990; Goto & Fink, 1989; Creighton & Ewbank, 1994). Large multidomain proteins are relatively unexplored. One of the major interests of exploring large proteins is to study the effect of multiple independent domains on the unfolding−folding behavior and nature of the intermediate states.

Glutaminyl-tRNA synthetase is a large monomeric protein (MW 64 500) having four domains. The X-ray crystals structure of its complex with $tRNA^{Gln}$ and ATP has been solved (Rould *et al.*, 1989). It has been reported that ATP and $tRNA^{Gln}$ induce a significant conformational change indicating interdomain communication (Bhattacharyya & Roy, 1993). The protein and its mutants can be produced in large quantities (Perona *et al.*, 1988; Bhattacharyya *et al.*, 1991) with relative ease. Thus, glutaminyl-tRNA synthetase may be a good system to address many of the questions related to unfolding−folding behavior of large proteins.

In this article we report the urea induced equilibrium denaturation of glutaminyl-tRNA synthetase and show that a stable molten globule-like intermediate exists at low urea concentrations. We have been able to derive the relative stabilities and activation energy barriers from equilibrium studies and kinetics of unfolding.

MATERIALS AND METHODS

Materials. Ultrapure urea was purchased from Spectrochem (India). DTT, DTNB, apoferritin, alcohol dehydrogenase, BSA, ovalbumin, and α-lactalbumin were purchased from Sigma Chemical Co. (St. Louis, MO). ANS was purchased from Molecular Probes Inc. (Eugene, OR). All other chemicals were of analytical grade.

Enzyme Purification. Glutaminyl-tRNA synthetase was purified according to Bhattacharyya *et al.* (1991), and the concentration was determined using a $E_{280}^{1\%} = 10.2$ (Hoben *et al.*, 1982).

Spectroscopic Methods. Fluorescence measurements were made on a Hitachi F3010 spectrofluorometer. Tryptophan fluorescence emission spectra were measured at various urea concentrations in Tris-HCl buffer, pH 7.5, at protein concentrations of 1−2 μM. Excitation wavelength was at 295 nm, and the emission was monitored at 340 nm. The band pass was 3 nm for both excitation and emission unless otherwise mentioned. The temperature was controlled by

† This work was supported by a grant from the Council of Scientific and Industrial Research (India).

* To whom correspondence should be addressed. FAX: 91-33-343886; E-MAIL: siddarth@boseinst.ernet.in.

® Abstract published in *Advance ACS Abstracts,* March 15, 1995.

[1] Abbreviations: GlnRS, glutaminyl-tRNA synthetase; DTNB, dithiobis(2-nitrobenzoic acid); DTT, dithiothreitol; FPLC, fast protein liquid chromatography; CD, circular dichroism; UV, ultraviolet; V_{el}, elution volume; ANS, 1-anilino-8-naphthalenesulfonate; EDTA, ethylenediaminetetraacetic acid.

0006-2960/95/0434-5242$09.00/0

circulating water through the cell holder. For measurements containing ANS (30 μM), the excitation wavelength was 420 nm to avoid inner filter effect and the emission was monitored at 482 nm. Appropriate blank values were always subtracted from all measurements.

Circular dichroism (CD) spectral measurements in the near-UV and far-UV regions were made on a JASCO J-600 spectropolarimeter using a 0.1 cm path length cuvette for far-UV and 1.0 cm for the near-UV. Protein concentration was typically 1−2 μM for the far-UV and 10 μM for the near-UV CD.

Equilibrium and Kinetic Denaturation Studies. Urea denaturation experiments were performed by diluting the stock enzyme solution with different volumes of buffer (0.1 M Tris-HCl, pH 7.5) and a standard urea solution in the same buffer in such a way so as to attain the desired final enzyme and urea concentrations. The solutions were then incubated overnight to attain complete equilibrium. In kinetic experiments, the change in fluorescence emission or CD intensity was monitored within 15 s of the addition of the denaturant to the protein. When the fluorescence and CD values leveled off completely (usually by 1 h), that value was taken as F_∞ or Y_∞. The kinetic data were plotted as $\ln(F_t - F_\infty)$ vs time. The kinetic experiments were done at urea concentrations well past the midpoints of the respective transitions. Under these conditions, absolute values of the initial slopes of the $\ln(F_t - F_\infty)$ vs time plot are equal to the reciprocal relaxation time (Ikai & Tanford, 1973). Again, as all the points were done under strong denaturing conditions, where back reaction for the respective transitions is not significant for the initial times, the inverses of the relaxation times were taken as the forward rate constants of the respective transitions (Finn *et al.*, 1992). For unfolding rates monitored by CD, a three state model of N ↔ I ↔ U was assumed. Since the N → I transition (as monitored by fluorescence intensity) was considerably faster than the I → U transition monitored by CD at the same urea concentration, we made an assumption of rapid equilibrium for the N ↔ I step. Under such an assumption, the rate constants were calculated from the slope of the $\ln(Y_t - Y_\alpha)$ versus time plot.

Determination of Sulfhydryl Content. The progressive exposure of the cysteines of glutaminyl-tRNA synthetase was followed at increasing denaturant concentrations by reaction with DTNB. The protein solution was incubated overnight in different urea concentrations in deaereated 0.1 M Tris-HCl buffer, pH 7.5, containing 1 mM EDTA to prevent aerial oxidation of the reactive sulfhydryls. The DTNB reactions were done at 25 °C in the presence of 1 mM DTNB. The protein concentration used was 2 μM. An equal volume of DTNB solution was added to the reference cuvette which contained everything except the protein. The liberated 2-nitro-5-mercaptobenzoic acid was determined at 412 nm after 1 h. A molar extinction coefficient of 13.6×10^3 cm^{-1} M^{-1} was used (Ellman, 1959).

Size-Exclusion Chromatography. To determine the compactness of the intermediate state, Stokes radii of the native, the intermediate, and the denatured states were determined by size-exclusion chromatography (FPLC) on Superose 12 (1.0 × 30 cm) at 25 °C. The column was equilibrated with 0.1 M Tris-HCl, pH 7.5 buffer containing different concentrations of urea. The glutaminyl-tRNA synthetase was incubated overnight at a final concentration of 2 μM protein at a given urea concentration as described above, and 100 μL was injected onto the Superose 12 column equlibrated with the same buffer, containing the same concentrations of urea. The column was calibrated with proteins of known Stokes radii in buffer containing no urea. Uversky (1993) has shown that Superose 12 column elution properties show no significant change in a wide range of urea concentrations. Apoferritin, alcohol dehydrogenase, bovine serum albumin, ovalbumin, and α-lactalbumin were used for calibration. The Stokes radii of glutaminyl-tRNA synthetase under different conditions were determined from a plot of Stokes radius of known proteins versus the elution volume.

Nonlinear Least Squares Fitting of the Equilibrium Spectroscopic Data. The equilibrium denaturation data (both fluorescence intensity and CD) were fitted to the following equation:

$$S_{obs} = \frac{S_N}{[1 + e^{-(\Delta G_1 + m_1[D])/RT}][1 + e^{-(\Delta G_1 + m_2[D])/RT}]} + \frac{S_I}{1 + [e^{-(\Delta G_1 + m_1[D])/RT}] + [e^{-(\Delta G_2 + m_2[D])/RT}]} + \frac{S_U}{[1 + e^{(\Delta G_2 + m_2[D])/RT}][1 + e^{(\Delta G_1 + m_1[D])/RT}]}$$

where S_N, S_I, and S_U represent respectively the signal intensities of the native, the intermediate, and the unfolded state. R is the gas constant and T is the absolute temperature.

The equation was derived assuming one intermediate (N ↔ I ↔ U) state. The variation of ΔG with denaturant concentration was assumed to be linear, $\Delta G_1 = \Delta G°_1 + m_1[D]$. Five independent parameters, ΔG_1, ΔG_2, m_1, m_2, and S_I (ΔG_1 is the free energy difference between the native and the intermediate states, ΔG_2 is the free energy difference between the native and the unfolded states, m_1 is the slope of the first transition, m_2 is the slope of the second transition and S_I is the value of the spectroscopic parameter for the pure intermediate state), were systematically varied over a range of values, and χ^2 values were determined. The set of values that gave the minimum χ^2 was assumed to be the best fit curve (χ^2 is defined as $\sum(Y_f - Y)^2/Y_f$, where Y is the observed value and Y_f is the corresponding value of Y with a set of fitted parameters).

RESULTS

Fluorescence intensity and emission maximum of the tryptophan residues of proteins are sensitive probes for protein denaturation. Glutaminyl-tRNA synthetase has seven tryptophan residues, and they are distributed throughout the molecule. Their positions are 87, 92, 205, 242, 285, 386, and 458 in the sequence (Yamao *et al.*, 1982). Thus, they are distributed in all the domains (Rould *et al.*, 1989), although many are clustered in the N-terminal half. We have used the intensity and emission maximum of the tryptophan fluorescence as probes for urea induced denaturation of the protein. Figure 1 shows the emission spectra of glutaminyl-tRNA synthetase at different urea concentrations (0, 1.5, 2, 2.5, 4, and 6 M urea). It is clear from the spectra that there is a large decrease of fluorescence intensity between 0 and 2 M urea, but very little shift of emission maximum. At higher urea concentrations, the emission maximum shifts significantly without much change in the intensity. This

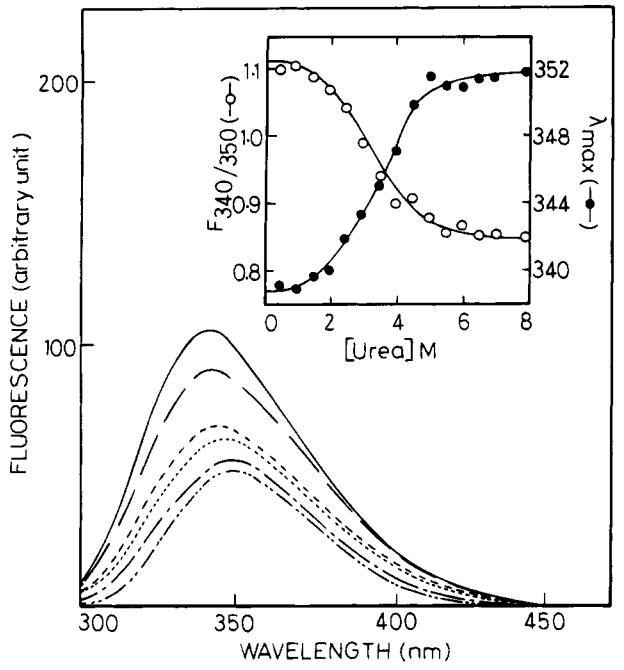

FIGURE 1: Effect of urea concentrations on the tryptophan fluorescence of GlnRS in 0.1 M Tris-HCl, pH 7.5. The excitation wavelength was 295 nm. Emission spectra in the presence of 0 M (—), 1.5 M (— —), 2.0 M (- - -), 2.5 M (•••), 4.0 M (— - —), and 6.0 M (— •• —) urea. The inset shows the $F_{340/350}$ ratio and wavelength maximum as a function of urea concentration. The band pass for both excitation and emission was 3 nm, and the temperature was 25 °C.

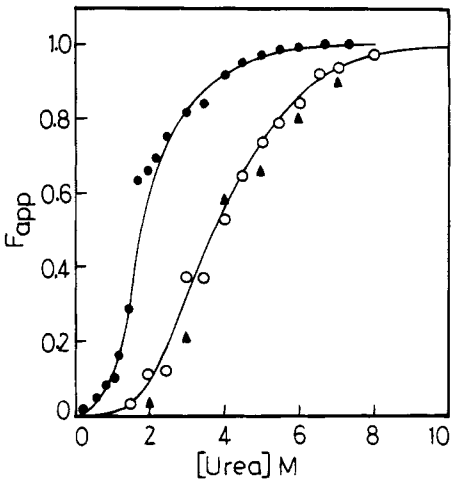

FIGURE 2: F_{app} versus urea concentration plot for urea induced unfolding of GlnRS by fluoerscence intensity (●) at 340 nm, far-UV CD (○) at 220 nm, and sulfhydryl reactivity (▲). All the experiments were done in 0.1 M Tris-HCl, pH 7.5 at 25 °C (except for SH reactivity determination which contained 1 mM EDTA in addition to the buffers described), after overnight incubation at respective urea concentrations to attain equilibrium. Sulfhydryl reactivities were determined spectrophotometrically at 412 nm using 1 mM DTNB. Far-UV CD was monitored at 220 nm using a 0.1 cm path length cuvette (2 μM glnRS), and four spectra were averaged to reduce the signal to noise ratio. Conditions for fluorescence measurements are as described in Figure 1.

suggests that two different transitions occur at lower and higher urea concentrations which affect predominantly the intensity and the emission maxima, respectively. Fluorescence intensity values drop sharply between 1 and 2 M urea and change slowly thereafter, finally leveling off at 6 M urea concentrations and beyond. The inset shows the emission maximum shift as a function of urea concentration. The emission maximum of the native glutaminyl-tRNA synthetase is 338.6 nm, which changes little (340 nm) up to 2 M urea; beyond that, there is a significant red shift of the emission maximum which finally levels off beyond 6 M urea to a value of 352 nm. A similar trend is seen for the F_{340}/F_{350} ratio, which also reflects the emission maximum shift. The approximate midpoint of transition is 3.5 M urea. This is significantly higher than the midpoint of transition of the fluorescence intensity change, which is around 1.7 M urea. The characteristic changes of fluorescence spectra upon incerase of urea concentration were found to be fully reversible (data not shown). Nonlinear least squares fit of the fluorescence intensity data fits well with two transitions, and the corresponding ΔG values are 9.8 ± 1.02 and 18.5 ± 0.73 kJ/mol.

We have also monitored the urea induced denaturation by far-UV CD and sulfhydryl reactivity. The far-UV CD intensity shows little change up to 2 M urea and then declines rapidly to approximately 20% of the initial value at 7 M urea. This indicates that the first transition causes only a small change in the CD signal, suggesting that most of the secondary structure in this transition remains intact. In contrast, most of the secondary structure is disrupted in the second transition. As described previously, this transition also causes large red shift of the emission maxima of the tryptophans, implying that this transition is a consequence of unfolding of the major part of the molecule. This midpoint of the transition is around 3.7 M urea. Nonlinear least squares fit of the CD data shows two transitions having ΔG values of 8.8 and 18.1 kJ/mol, in good agreement with the fluorescence data.

Glutaminyl-tRNA synthetase has ten cysteines, of which two are probably paired in a disulfide bond (Rould *et al.*, 1990). Of the remaining eight, only three are available for reaction with DTNB in the native state (Bhattacharyya & Roy, 1993). We have measured the reactivity of the cysteines as a function of urea concentration. The total number of reacted sulfhydryl groups was determined after 1 h of incubation with DTNB, and this may include some slower reacting sulfhydryls groups. Going from 0 to 2 M urea, only one additional cysteine becomes available for DTNB reaction whereas at higher urea concentrations increasingly more cysteines become available for titration by DTNB, with a final value approaching 8 titrable cysteines. The midpoint of the second transition (3.6 M urea) agrees fairly well with the midpoint of the transition obtained from CD data. This suggests that, at high urea concentrations, most of the molecule may be unfolded. The profile of number of titrable groups versus urea concentrations is consistent with two transitions in which the intermediate is native-like, whereas at high urea concentrations the protein is nearly completely unfolded. These data are summarized in Figure 2, which depicts the F_{app} values obtained from fluorescence intensity (F_{340}), far-UV CD signal at 220 nm, and the second transition of −SH reactivity against urea concentrations. It clearly demonstrates the existence of an intermediate state since the midpoints of the transitions, monitored by fluorescence intensity and CD/SH reactivity, are different. For transition monitored by fluorescence intensity, it is around 1.7 M urea, whereas far-UV CD and sulfhydryl reactivity gave a midpoint of around 3.7 M urea.

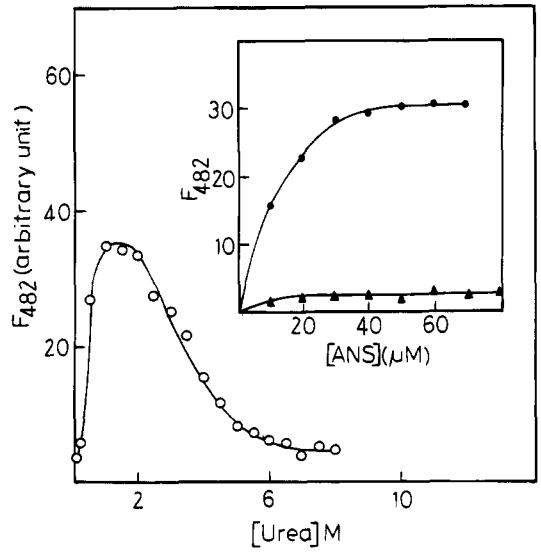

FIGURE 3: ANS binding: Change in intensity of fluorescence (F_{482}) in the presence of 2 μM GlnRS with increasing concentrations of urea in 0.1 M Tris-HCl, pH 7.5. The ANS concentration was 30 μM. In the inset, ANS fluorescence at 482 nm in the presence of 0 (▲) and 2 M (●) urea is plotted versus ANS concentrations. GlnRS concentration was 2 μM. The excitation wavelength was 420 nm, and the band pass was 3 nm, both for excitation and emission. The temperature was 25 °C.

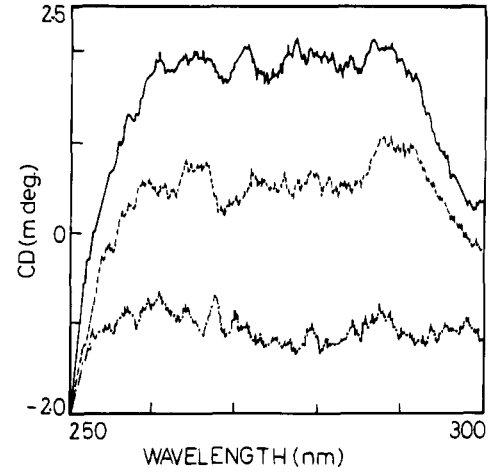

FIGURE 4: Near-UV CD spectra of GlnRS (10 μM) in the native form (—) and in the presence of 2 M (- - -) and 6 M (— • —) urea in 0.1 M Tris-HCl, pH 7.5 at 25 °C. The path length was 1.0 cm. Number of averaged spectra were 6.

The large loss of fluorescence intensity and small change of far-UV CD signal are often seen in transitions of native structures to molten globule states (Ptitisyn, 1992). In order to see whether the intermediate state is a molten globule, we have looked at the ANS binding to this intermediate state. One of the characteristic features of the molten globule state is increased access to interior hydrophobic patches by hydrophobic probes, such as ANS and bis-ANS (Semisotnov *et al.*, 1991; Rodionova *et al.*, 1989). Figure 3 shows the binding of 30 μM ANS to glutaminyl-tRNA synthetase as a function of urea concentration. As free ANS does not contribute significantly to the total fluorescence, the fluorescence intensity is a reflection of the bound ANS. The fluorescence intensity rapidly increases up to 2 M urea concentration and then declines slowly with a midpoint of transition around 3.5 M urea. This suggests that the intermediate is a potent binder of ANS, whereas the denatured state is a relatively poor binder. The molten globule states have been shown to bind an increased amount of ANS due to increased accessibility of the interior hydrophobic residues. The increased fluorescence may be due to increased affinity, increased quantum yield, or increased stoichiometry of binding. Figure 3 inset shows the ANS titration of glutaminyl-tRNA synthetase at native and 2 M urea concentration. At both 0 and 2 M urea concentrations, the binding of ANS shows saturation behavior, with similar midpoint of transitions. The final value at saturation is much higher at 2 M urea than for no urea. This indicates that binding affinity is not grossly different in the native state and the intermediate. Since the affinity is similar, the increased fluorescence may be due to increased quantum yield, increased number of binding sites, or both. The quantum yield of ANS, as well as the emission maximum, is known to be directly related to the degree of environmental polarity. In this case, emission maximum of native and intermediates bound ANS is not significantly different (around 485 nm; data not shown). This suggests that the difference in polarity of environment may not totally account for such a large increase of ANS fluorescence and hence increased binding stoichiometry may be a major factor. Such increased binding is consistent with the suggested nature of the intermediate state, that is, the molten globule. Thus, the data are consistent with increased accessiblity of the interior hydrophobic sites.

The molten globule states in smaller proteins are now fairly well characterized. In all cases, they retain native-like secondary structures but lose many of the tertiary interactions that give the protein interiors a solid-like characteristic. Such states show increased rotational freedom of the interior side chains, which leads to vanishing or greatly reduced side chain CD (Nozaka *et al.*, 1978; Dolgikh *et al.*, 1985), while retaining most of the far-UV CD characteristic of native-like secondary structure. Figure 4 shows the near-UV side chain CD of glutaminyl-tRNA synthetase without urea and at 2 and 6 M urea concentrations. The native protein shows distinct positive side chain CD, whereas it is totally absent in the 6 M urea denatured state. At 2 M urea the signal is greatly reduced, but even after making corrections for the possible noncompletion of the transition, a significant amount of side chain CD remains. We estimate by extrapolation that 50−60% of the initial CD signal may be lost upon complete conversion of the native state to the intermediate state. This may be interpreted as a loss of tertiary interactions of the large part of the molecule, although we do not rule out the possibility that some part of the molecule may still retain the tertiary structure.

Hydrodynamic properties of the intermediate state are of importance in trying to characterize the nature of the state. We have used size-exclusion FPLC to determine the Stokes radii of the native, the intermediate, and the denatured state. The experiment was carried out at low protein concentrations to avoid aggregation problems characteristic of many molten globule states (Gress *et al.*, 1994). Figure 5 shows the elution profile of glutaminyl-tRNA synthetase at three different urea concentrations, 0, 2, and 6 M. The elution volumes at 0, 2, and 6 M concentrations are 12, 11.7, and 9.9 mL, respectively. It is clear that the intermediate has an elution volume which is very similar to that of the native form. The corresponding Stokes radii are 3.6, 3.8, and 6 nm, indicating that the hydrodynamic property of the intermediate state is

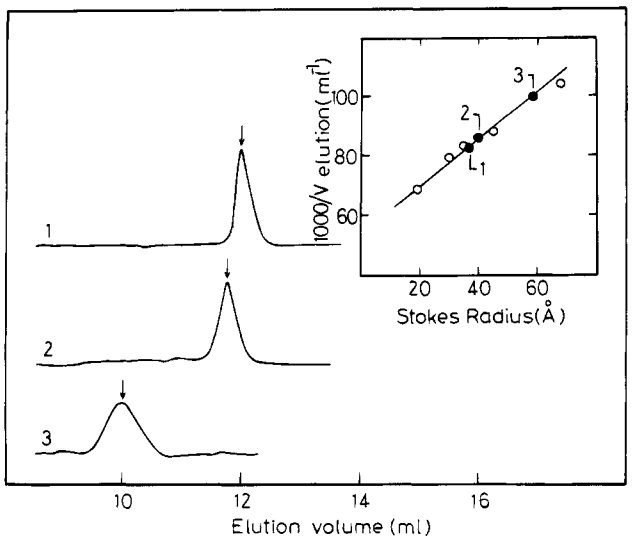

FIGURE 5: Elution profiles from size-exclusion column obtained for the GlnRS (1) in the absence of urea and in the presence of (2) 2 M and (3) 6 M urea. The column (Superose 12) equilibrated in 0.1 M Tris, pH 7.5, and the same buffer containing 2 and 6 M urea. The inset shows the dependence of migration rate ($1000/V_{el}$) of standard proteins on their Stokes radii (O) and GlnRS in absence of urea (1) and in the presence of (2) 2 M and (3) 6 M urea. The flow rate was 24 mL/h at 25 °C. The standard proteins used, in order of increasing Stokes radius, are α-lactalbumin, ovalbumin, BSA, alcohol dehydrogenase, and apoferritin.

very similar to that of the native state. Such compact native-like sizes are characteristic of the molten globule state.

The experiments described above establish that a stable intermediate exists in low urea concentrations, which is mostly in a molten globule-like state. Kinetics of denaturant induced unfolding can give valuable information on native state homogeneity and activation energy barrier. The interpretation of kinetic data is model dependent. We make the reasonable assumption that the kinetic scheme is N → I → U. As mentioned above, major fluorescence intensity change occurs in going from the native to the intermediate state, whereas far-UV CD change occurs primarily in transition from the intermediate to the denatured state. Thus, if the kinetics of unfolding is monitored by fluorescence intensity change, then the transition from the native state would be monitored predominantly. On the other hand, if far-UV CD is used to monitor the unfolding kinetics, then the transition to the unfolded state would be monitored predominantly. The $\ln(F_t - F_\infty)$ versus time plots were linear for all urea concentrations studied (data not shown). The absolute value of the slope of the line is equal to the reciprocal relaxation time of the transition, as urea concentrations are well past the midpoints of respective transitions and back reactions will not significantly influence the first part of the curve (Finn *et al.*, 1992). Figure 6 shows a plot of the natural logarithm of the relaxation times versus urea concentrations as monitored by CD and fluorescence intensity. The relaxation times as monitored by CD and fluorescence are distinctly different, indicating that they are indeed monitoring different steps.

The relationships of relaxation times with microscopic rate constants are model dependent. If the denaturant concentrations are chosen such that they are always well beyond the midpoint of transition, that is, in strong denaturing conditions, then the relaxation time reduces to the inverse of the rate constant of the transition being monitored. For fluorescence

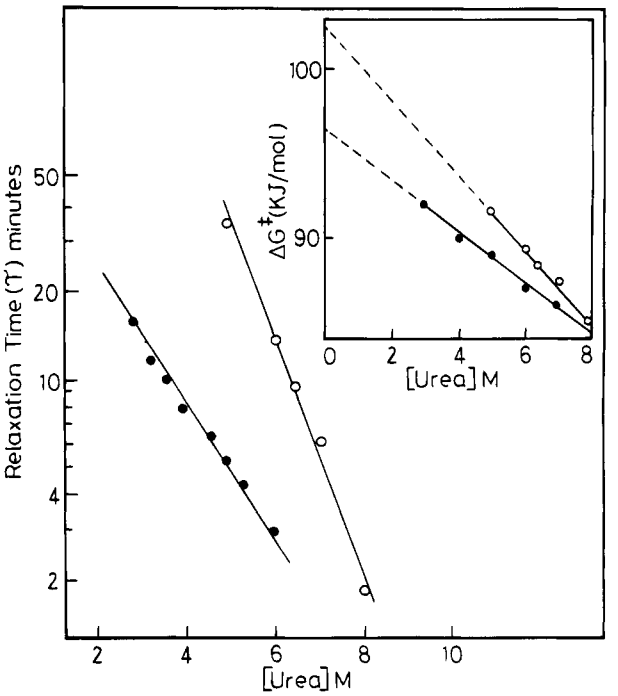

FIGURE 6: A semilog plot of the urea concentration dependence of the relaxation time monitored by fluorescence (●) and CD (O). Kinetics of unfolding of GlnRS was monitored by CD at 220 nm at urea concentrations of 5.0, 6.0, 6.5, 7.0, and 8.0 M urea. Kinetics of unfolding by loss of fluorescence emission intensity was monitored at 340 nm (excitation at 295 nm) at urea concentrations of 3.0, 4.0, 5.0, 6.0, and 7.0 M urea. Band passes were 3 nm for both excitation and emission. Experiments were done in 0.1 M Tris-HCl, pH 7.5 at 25 °C. The inset shows the plot of $\Delta G^{\ddagger}$ versus urea concentrations obtained from CD (O) and fluorescence intensity measurements (●).

monitored transition, this will be the N → I step (Finn, *et al.*, 1992), and in the case of the CD monitored transition, it will be the I → U step (see Materials and Methods). The relaxation time then can be correlated with the inverse of rate constant of the corresponding step. The rate constant (k) and the corresponding activation energy ($\Delta G^{\ddagger}$), thus derived at different urea concentrations, can be used to extrapolate to zero urea concentration to obtain activation energy ($\Delta G^{\ddagger}_{H_2O}$) of the respective steps (Finn *et al.*, 1992). The equations are:

$$\Delta G^{\ddagger} = -RT \ln(kh/K_\beta T) \quad (1)$$

$$\Delta G^{\ddagger} = \Delta G^{\ddagger}_{H_2O} + m[D] \quad (2)$$

where h, K_β, and R are the Planck, Boltzmann, and gas constants, respectively, and T is the absolute temperature. m and [D] are the slope and urea concentration, respectively. The inset of Figure 6 shows the extrapolation of activation energy obtained at different urea concentrations to zero urea concentration. The activation energy barriers between the N and I state are 96.2 ± 0.8 kJ/mol and for the I and U state, 102 kJ/mol.

DISCUSSION

The molten globule states of many small proteins have been studied; however, very few large multidomain proteins have been studied in this manner. We have studied equilibrium denaturation of the glutaminyl-tRNA synthetase,

which is a monomeric protein of 64.5 kDa having four distinct domains (Rould *et al.*, 1989). Several probes, such as far-UV CD, fluorescence, and sulfhydryl reactivity, have been used to characterize the urea induced denaturation. The noncoincidence of F_{app} plots, when followed by fluorescence intensity on the one hand and far-UV CD and sulfhydryl reactivity on the other, and the existence of an inflexion point clearly suggest the presence of one intermediate. Nonlinear least squares fitting indicated that inclusion of one intermediate is sufficient to produce a good fit, and the data are consistent with the existence of only one intermediate.

Size-exclusion FPLC suggests that this intermediate is compact and has a native-like Stokes radius. The hydrophobic probe ANS showed many-fold increased binding to this state compared to the native and the denatured states. Near-UV side chain CD suggests that the major part of tertiary structure may be disrupted. All these results suggest that at least a major part of the molecule may be in a molten globule-like state.

In hsp70, Palleros *et al.* (1993) detected a molten globule intermediate whose Stokes radius increases monotonically with increased urea concentration, resulting in continuous shift in elution volume. No such behavior is seen in glutaminyl-tRNA synthetase, where the elution volume of the molten globule state remains almost unchanged with increase in urea concentration.

Urea induced unfolding kinetics of glutaminyl-tRNA synthetase detected by fluorescence intensity and far-UV CD are significantly different. This is not unexpected, since the fluorescence and the CD changes are largely caused by different steps in the N ⇔ I ⇔ U pathway. The linearity of $\ln(Y_t - Y_\infty)$ vs time plot relfects the homogeneity of the native state, suggesting that no significant parallel reactions occur. The equilibrium data for change in tryptophan fluorescence intensity show that a large change occurs in the native to intermediate transition and much less change for intermediate to unfolded transition. Thus, the unfolding kinetics monitored by fluorescence intensity change at each urea concentration was interpreted as conversion from the native to the intermediate state (N ⇀ I), and a $\Delta G^{\ddagger}$ value of 96.2 ± 0.8 kJ/mol was obtained. Similarly, the unfolding kinetics monitored by CD signal yields an activation energy barrier value of 102 kJ/mol for the second step (I ↔ U). The deduced activation energies for the molten globule-like intermediate state are fairly high but not incompatible with other studies (Baker *et al.*, 1992).

In conclusion, we have demonstrated the existence of a urea induced molten globule state in a large multidomain protein which is separated from the native and the denatured state by high activation energy barriers.

REFERENCES

Baker, D., Sohl, J., & Agard, D. A. (1992) *Nature, 356*, 263−265.

Baldwin, R. L. (1991) *Chemtracts: Biochem. Mol. Biol. 2*, 379−389.

Baum, J., Dobson, C. M., Evans, P. A., & Hanly, C. (1989) *Biochemistry 28*, 7−13.

Bhattacharyya, T., & Roy, S. (1993) *Biochemistry 32*, 9268−9273.

Bhattacharyya, T., Bhattacharyya, A., & Roy, S. (1991) *Eur. J. Biochem. 200*, 729−745.

Christensen, H., & Pain, R. H. (1991) *Eur. Biophys. J. 19*, 221−229.

Creighton, T. E., & Ewbank, J. J. (1994) *Biochemistry 33*, 1534−1538.

Damaschun, G., Gernet, C., Damaschun, H., Bychkova, V. E., & Ptitsyn, O. B. (1986) *Int. J. Biol. Macromol. 8*, 226−230.

Dobson, C. M. (1992) *Curr. Opin. Struct. Biol. 2*, 6−12.

Dolgikh, D. A., Gilmanshin, R. I., Brazhinikov, E. V., Bychkova, V. E., Semisotonov, G. V., Venyaminov, S. Y., & Ptitsyn, O. B. (1981) *FEBS Lett. 136*, 311−315.

Dolgikh, D. A., Abaturov, L. V., Bolotina, I. A., Brazhnikov, E. V., Bychkova, V. E., Bushuev, V. N., Gilmanshin, R. L., Lebedev, Yu. O., Semisotnov, G. V., Tiktopulo, E. I., & Ptitsyn, O. B. (1985) *Eur. Biophys. J. 13*, 109−121.

Ellman, G. L. (1959) *Arch. Biochem. Biophys. 82*, 70−77.

Ewbank, J. J., & Creighton, T. E. (1991) *Nature 350*, 518−520.

Fink, A. L., Calciano, L. J., Goto, Y., & Palleros, D. R. (1991) In *Conformation and forces in protein folding* (Nall, B. T., & Dill, K. A., Eds.) pp 169−174, AAAS, Washington, DC.

Fink, A. L., Calciano, L. J., Goto, Y., Nishimura, M., & Swedberg, S. A. (1993) *Protein Sci. 2*, 1155−1160.

Finn, E. B., Chem. X., Jennings, P. A., Soalau-Bethell, S. M., & Mathews, C. R. (1992) In *Protein Engineering* (Rees, A. R., Sternberg, M. J. E., & Wetzel, R., Eds.) pp 167−189, Oxoford University Press, New York.

Gast, K., Zirwer, D., Welfle, H., Bychkova, V. E., & Ptitsyn, O. B. (1986) *Int. J. Biol. Macromol. 8*, 231−236.

Goto, Y., & Fink, A. L. (1989) *Biochemistry 28*, 945−952.

Goto, Y., & Fink, A. L. (1990) *J. Mol. Biol. 214*, 803−805.

Gress, J. O. B., Marquis-Omer, D., Middaugh, C. R., & Sanyal, G. (1994) *Biochemistry 33*, 2620−2627.

Hoben, P., Royal, N., Cheung, A., Yamao, F., Biemann, K., & Soll, D. (1982) *J. Biol. Chem. 257*, 11644−11650.

Ikai, A., & Tanford, C. (1973) *J. Mol. Biol. 73*, 145.

Jagannadham, M. V., & Balsubhramanian, D. (1985) *FEBS Lett. 188*, 326−330.

Jeng, M. F., & Englander, S. W. (1991) *J. Mol. Biol. 221*, 1045−1061.

Jeng, M. F., Englander, S. W., Elove, G. A., Wand, A. J., & Roder, H. (1990) *Biochemistry 29*, 10433−10437.

Khurana, R., & Udgaonkar, J. B. (1993) *Biochemistry 33*, 106−115.

Kim, J., & Kim, H. (1986) *Biochemistry 25*, 7867−7874.

Kuwajima, K. (1989) *Proteins: Struct., Funct., Genet. 6*, 87−103.

Lehrman, S. R., Tuls, J. L., Havel, H. A., Haskell, R. J., Putman, S. D., & Tomich, C. S. C. (1991) *Biochemistry 30*, 5777−5784.

Mitaku, S., Ishidu, S., Hirano, Y., Itoh, H., Kataoka, R., & Saito, N. (1991) *Biophys. Chem. 40*, 21−22.

Nozaka, M., Kuwajima, K., Nitta, K., & Sugai, S. (1978) *Biochemistry 17*, 3753−3758.

Palleros, D. R., Katherine, L. S., & Fink, A. L. (1993) *Biochemistry 32*, 4314−4321.

Permyakov, E. A., Grischenko, V. M., *Kalinichenko*, L. P., Orlov, N. Y., Kuwajima, K., & Sugai, S. (1991) *Biophys. Chem. 34*, 55−62.

Perona, J. J., Swanson, R., Steitz, T. A., & Soll, D. (1988) *J. Mol. Biol. 202*, 121−126.

Ptitsyn, O. B. (1987) *J. Protein Chem. 6*, 273−293.

Ptitsyn, O. B. (1992) In *Protein Folding* (Creighton, T. E., Ed.) pp 243−300, W. H. Freeman & Co., New York.

Ptitsyn, O. B., Pain, R. H., Semisotnov, G. V., Zerovnik, E., & Razgulyaev, O. I. (1990) *FEBS Lett. 262*, 20−24.

Rodionova, N. A., Semisotnov, G. V., Kutyshenko, V. P., Uversky, V. N., Bolotina, I. A., Bychkova, V. E., & Ptitsyn, O. B. (1989) *Mol. Biol. (Moscow) 23*, 683−692.

Rould, M. A., Perona, J. J., Soll, D., & Steitz, T. A. (1989) *Science 246*, 1135−1142.

Semisotnov, G. V., Rodionova, N. A., & Razgulyaev, O. I. (1991) *Biopolymer 31*, 119−128.

Uversky, V. N. (1993) *Biochemistry 37*, 13288−13298.

Uversky, V. N., Semisotnov, G. V., Pain, R. H., & Ptitsyn, O. B. (1992) *FEBS Lett. 344*, 89.

Yamao, F., Inokuchi, H., Cheung, A., Ozeki, H., & Soll, D. (1982) *J. Biol. Chem. 257*, 11639−11643.

BI942408C